
Collective Instabilities

2.1 Overview

Charged beam particles in a storage ring interact with the surrounding walls of the vacuum chamber and create electromagnetic fields that can act back on the particles themselves. These fields disturb their intended longitudinal and transverse position given by the magnetic guide fields and the electromagnetic radio-frequency (rf) fields. If, in turn, the disturbed particles create fields that tend to enhance the disturbed motion, a “collective instability” occurs. This must not be confused with disturbed particle trajectories due to optical resonances or nonlinear components of the guide field, which are not of a collective nature.

Collective instabilities show up as longitudinal or transverse beam excitations, where individual bunches or parts of bunches oscillate against each other. These oscillations may remain limited in amplitude, they may rise and collapse irregularly or periodically (sometimes in a sawtooth fashion), or they may increase in amplitude until the beam is lost.

Beam instabilities impair the quality of synchrotron radiation. One important figure of merit is the brilliance or spectral brightness¹ B :

$$B = \frac{\dot{N}_\gamma}{4\pi^2 \sigma_x \sigma_y \sigma_{x'} \sigma_{y'} dE/E_\gamma} \left(\frac{\text{photons s}^{-1}}{\text{mm}^2 \text{ mrad}^2 \text{ 0.1\% bandwidth}} \right), \quad (2.1)$$

where σ_x , σ_y , $\sigma_{x'}$ and $\sigma_{y'}$ are standard deviations of the horizontal and vertical spatial and angular distributions, respectively. By convention, the photon flux \dot{N}_γ is integrated over a photon energy range (“bandwidth”) of $dE/E_\gamma = 0.001$ or 0.1%. Instabilities limit the brilliance in different ways:

¹ The term “brilliance” tends to be more popular in Europe. Depending on the author, “brightness” may denote the photon flux per bandwidth and solid angle, or the photon flux per area and solid angle; whereas “spectral brightness” is synonymous with brilliance. To increase the confusion, these quantities may or may not be normalized to the electron beam current.

- A transverse oscillation of electron bunches increases the time-averaged size and angular divergence of the radiation source.
- An oscillation in longitudinal phase space implies an oscillation of the electron energy E , which increases the time-averaged spread of photon energies in the undulator line spectrum, since the photon energy of undulator radiation is proportional to E^2 .
- Instabilities can be a serious limitation of the storable beam current I and consequently of the photon flux $\dot{N}_\gamma \sim I$.

It is instructive and for many applications sufficient to describe the longitudinal or transverse motion as a harmonic oscillation

$$A(t) = A_0 \exp(-i[\Omega + \Delta\Omega]t) . \quad (2.2)$$

The frequency shift $\Delta\Omega$ is a complex number. Its real part describes a modification of the oscillation frequency, whereas its imaginary part denotes the rate of change of the oscillation amplitude. The signature of an instability is an increasing amplitude, the imaginary part of $\Delta\Omega$ being positive.

For electrons travelling nearly at the speed of light, the electromagnetic fields created by the interaction with the surrounding walls act almost exclusively on trailing electrons, and they are figuratively called *wake* fields. In a storage ring, however, an electron can be influenced by the wake field of trailing particles from previous revolutions.

Instead of fully characterizing the wake field created by a given charge at each point in space and time, it is usually sufficient to specify the voltage experienced by a trailing “test” charge as function of its distance to the leading charge, integrated over a certain period of time (e.g. the time it takes to traverse significant structures like rf cavities). The Fourier transform of this (real) wake function is a complex function of frequency. This function is called *impedance*. In principle, impedance and wake function are equivalent descriptions of the same reality, one given in the frequency domain, the other in the time domain. Their usage, however, depends on the respective application. The wake function, for example, is better suited for time-dependent simulations, whereas analytical calculations are often simpler in the frequency domain since the beam motion is periodic and certain parameters (like the skin depth in the wall of a vacuum chamber) depend on frequency.

Impedance, wake function and the beam instabilities caused by them can be classified according to the following criteria:

- *Longitudinal* wake fields influence the energy of beam particles and their spatial distribution along the beam axis. *Transverse* wake fields deflect beam particles perpendicular to the beam axis in horizontal or vertical direction. Consequently, there are longitudinal and transverse wake functions, impedances and instabilities.

- *Long-range* wake fields decay slowly enough to act on trailing particle bunches. They correspond to *narrow-band* impedances in the frequency domain. They may decay over many revolution times of the storage ring causing *multi-bunch* instabilities where all bunches act like an ensemble of coupled pendula.
Short-range wake fields correspond to *broad-band* impedances and are, by definition, only significant within a particle bunch. Oscillations within a bunch are called *single-bunch* instabilities.
- There are distinct differences between beam instabilities in *linear accelerators* and *storage rings* as well as between oscillations of a *continuous beam* (also called *coasting beam*) and a *bunched beam*.

Concentrating on synchrotron radiation sources, this book is restricted to instabilities of bunched beams in storage rings. Under ordinary circumstances, only two types of instabilities are significant:

- “*Robinson*”-*type instabilities* are predominantly multi-bunch oscillations. The forces resulting from long-range wake fields create an imaginary frequency shift that is proportional to the beam current. This kind of instability exists at all values of beam current without any threshold. In practice, however, a threshold is given by the current above which the rise time of the instability is shorter than the damping time of stabilizing mechanisms (see Sect. 2.5). This instability type can essentially be understood using a one-particle model where each bunch is represented by a “macro particles”.
- *Mode-coupling instabilities* are single-bunch phenomena. Their model description requires to split a bunch into two or more macro particles, or to treat it as a continuous charge distribution. At low bunch current, the wake fields cause a current-dependent shift of the real frequency of each mode of oscillation. A non-zero imaginary frequency shift, that describes an instability, occurs only above a certain threshold current at which the real frequencies of two modes merge.

An example of a phenomenon that does not quite fit into these two categories is the “fast” ion instability, which is addressed in Appendix G. So far, it was only unambiguously observed in experiments where the residual gas pressure was intentionally increased.

Viewed in the frequency domain, instabilities can occur when the impedance is non-zero at a frequency that corresponds to a possible oscillation mode of the electron beam. Therefore, the frequency spectrum of a beam is described next. What follows is an introduction to wake functions and impedances, and how to predict them. Subsequently, different instability models with increasing degree of complexity are discussed, followed by a description of “natural” damping mechanisms. Finally, methods to measure the impedance at storage rings are addressed. The active control of collective instabilities using feedback systems is the topic of a later chapter.

2.2 The Frequency Spectrum of a Stored Beam

The beam spectrum, i.e. the beam current as function of frequency is deduced from the current as function of time, detected at a fixed position of the storage ring. This is analogous to the impedance, which is usually linked to geometrical or electrical properties at a fixed position of the vacuum vessel. Oscillations of the electron bunches create additional lines in the beam spectrum. Their frequencies depend not only on the oscillation frequency but also on the phase differences between subsequent bunches. Excitation of a particular oscillation requires an impedance component at its frequency to be present.

The beam spectrum $J(\omega)$ and the beam current as function of time $j(t)$ are connected via Fourier transform:

$$\begin{aligned} J(\omega) &= \int_{-\infty}^{\infty} dt j(t) \exp(-i\omega t), \\ j(t) &= \frac{1}{2\pi} \int_{-\infty}^{\infty} d\omega J(\omega) \exp(i\omega t). \end{aligned} \quad (2.3)$$

The notion of a negative frequency² should not create any conceptual difficulty considering that only the real part of the oscillation is measurable:

$$\operatorname{Re} \exp(-i\omega t) = \operatorname{Re} \exp(i\omega t) = \cos(\omega t). \quad (2.4)$$

Thus, a measuring apparatus (e.g. a spectrum analyzer) does not distinguish between negative and positive frequencies. The negative part of a spectrum may be thought of as being “flipped over” to the positive side of the frequency axis.

A measured spectrum also depends on the frequency characteristics of the detector and electronic circuitry. In the following description of idealized spectra, technical issues of this kind are ignored. A more detailed discussion of beam spectra is given e.g. in [2], instruments like spectrum analyzers and network analyzers are explained in [3].

2.2.1 Pointlike Electron Bunches

As a starting point, consider a beam of pointlike electron bunches without any longitudinal or transverse oscillation (see Fig. 2.1).

Case 1a. Let a pointlike electron bunch make a single passage past a (likewise pointlike) detector. The current signal (in arbitrary units) can be described using Dirac’s δ -function

$$j(t) = \delta(t). \quad (2.5)$$

² Throughout this book, f denotes the frequency in terms of cycles per time unit, whereas $\omega = 2\pi f$ is the angular frequency, i.e. phase angle per time unit. For simplicity, the word “frequency” is used for both.

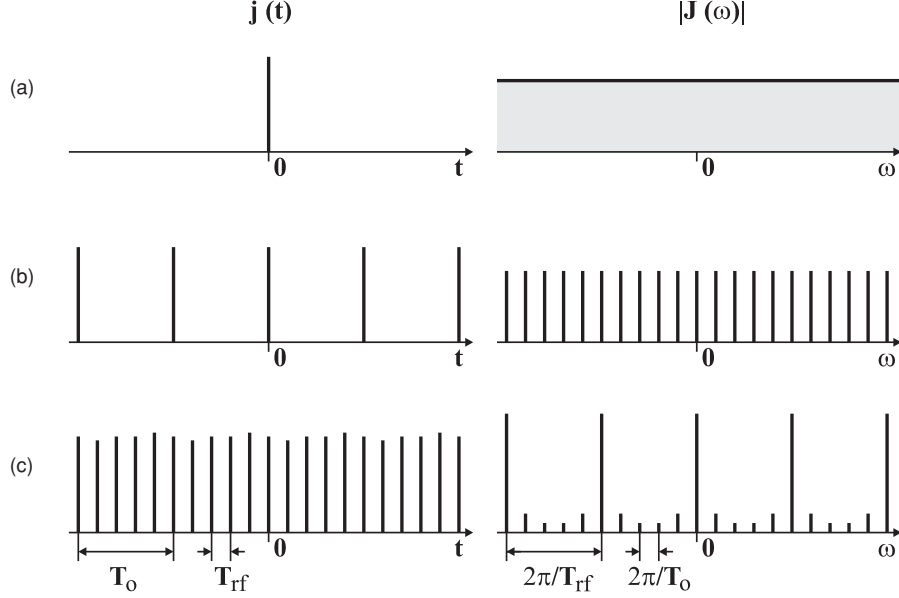


Fig. 2.1. Detected current signal caused by pointlike electron bunches as function of time (*left*) and frequency (*right*). (a) Single passage and (b) multiple passages of a single bunch with revolution time T_o , (c) multiple passages of T_o/T_{rf} equidistant bunches. Slight differences in bunch charge cause spurious revolution harmonics between the dominant rf harmonics

Fourier transformation results in an infinitely broad spectrum:

$$J(\omega) = \int_{-\infty}^{\infty} dt \delta(t) \exp(-i\omega t) = 1. \quad (2.6)$$

Case 1b. Let a pointlike electron bunch circulate in a storage ring with revolution time T_o and revolution frequency $\omega_o = 2\pi/T_o$. The beam current as function of time corresponds to a sequence of equidistant δ -functions:

$$j(t) = \sum_{n=-\infty}^{\infty} \delta(t - nT_o). \quad (2.7)$$

Its Fourier transform is

$$J(\omega) = \sum_{n=-\infty}^{\infty} \exp(-i\omega nT_o) = \omega_o \sum_{p=-\infty}^{\infty} \delta(\omega - p\omega_o), \quad (2.8)$$

where Poisson's sum rule for Fourier pairs $[f(t), F(\omega)]$ (e.g. [4])

$$\sum_{n=-\infty}^{\infty} f(an) = \frac{1}{a} \sum_{p=-\infty}^{\infty} F\left(\frac{2\pi p}{a}\right) \quad (2.9)$$

was applied with $f = \exp(-i\omega n T_o)$ and $a = T_o$. The electron bunch in the storage ring creates a spectrum of lines at integer multiples of the revolution frequency. These lines may be called “revolution harmonics”. In order to understand this result qualitatively, consider (2.7) to represent periodic samples of a sinewave. These samples are consistent with an oscillation of frequency ω_o , but any integer multiple frequency would yield the same sample values. This frequency ambiguity is called “aliasing”.

Case 1c. With $\omega_{\text{rf}} = h\omega_o$ being the rf frequency, h electron bunches correspond to a complete fill of the storage ring in the sense that each rf potential well (also called “bucket”) is occupied, and h is called the harmonic number of the storage ring. The current given by pointlike bunches with a temporal spacing of $T_{\text{rf}} = T_o/h$ is

$$j(t) = \sum_{n=-\infty}^{\infty} \delta(t - nT_{\text{rf}}) . \quad (2.10)$$

In analogy to (2.8), the beam spectrum is given by

$$J(\omega) = h\omega_o \sum_{p=-\infty}^{\infty} \delta(\omega - p\omega_{\text{rf}}) , \quad (2.11)$$

In this case, the lines of the spectrum are at integer multiples of the rf frequency and may be called “rf harmonics”. In real storage rings, however, small inhomogeneities in the fill pattern create spurious lines at multiples of the revolution frequency ω_o as well.

2.2.2 Extended Electron Bunches

The unphysical result of a spectrum extending to infinite frequency is a consequence of the assumption of pointlike bunches. As a more realistic approach, let the longitudinal charge density of each electron bunch be a Gaussian with standard deviation σ_τ in units of time (see Fig. 2.2).

Case 2a. A bunch with Gaussian charge distribution that passes the detector only once creates a current signal (in arbitrary units) of

$$j(t) = \frac{1}{\sqrt{2\pi}\sigma_\tau} \exp(-t^2/2\sigma_\tau^2) \quad (2.12)$$

and its spectrum is given by

$$J(\omega) = \exp(-\omega^2\sigma_\tau^2/2) . \quad (2.13)$$

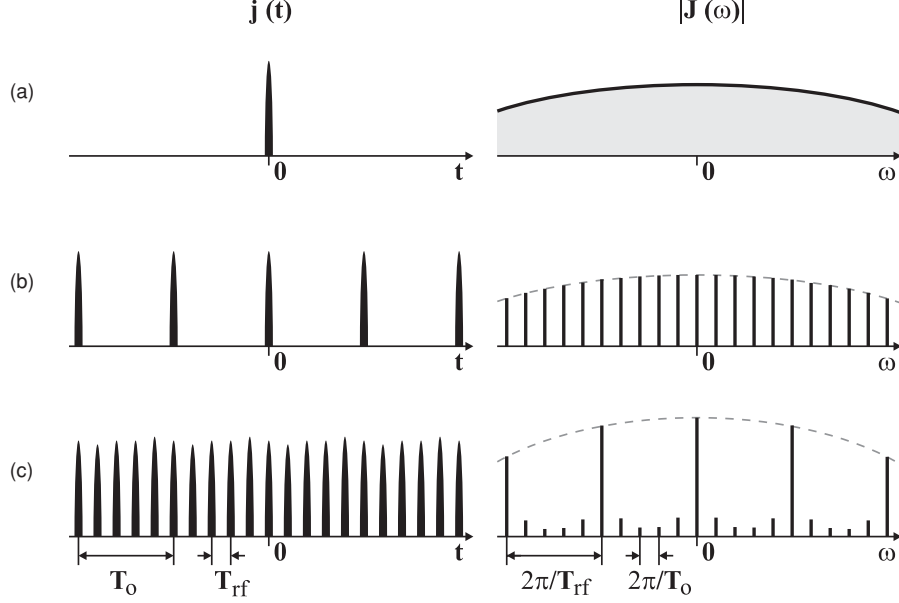


Fig. 2.2. Detected current signal caused by longitudinally extended bunches as function of time (*left*) and frequency (*right*). (a) Single passage and (b) multiple passages of a single bunch with revolution time T_0 , (c) multiple passages of T_0/T_{rf} equidistant bunches

Case 2b. For a Gaussian bunch in a storage ring with revolution time T_0 and revolution frequency $\omega_0 = 2\pi/T_0$, the beam current is a convolution of the previously assumed sequence of δ -functions and the charge density distribution:

$$\begin{aligned}
 j(t) &= \frac{1}{\sqrt{2\pi}\sigma_\tau} \sum_{n=-\infty}^{\infty} \int_{-\infty}^{\infty} dt' \delta(t' - nT_0) \exp(-[t - t']^2/2\sigma_\tau^2) \\
 &= \frac{1}{\sqrt{2\pi}\sigma_\tau} \sum_{n=-\infty}^{\infty} \exp(-[t - nT_0]^2/2\sigma_\tau^2). \quad (2.14)
 \end{aligned}$$

According to the convolution theorem, its Fourier transform is simply given by the product of the Fourier transforms of the convoluted functions:

$$J(\omega) = \omega_0 \exp(-\omega^2\sigma_\tau^2/2) \sum_{p=-\infty}^{\infty} \delta(\omega - p\omega_0). \quad (2.15)$$

The finite extension of the electron bunches defines the envelope of the line spectrum: the shorter the bunches, the broader the spectrum. The line width in the spectrum, on the other hand, is determined by the envelope of the distribution in time: the longer the measurement time (here assumed to be infinite), the smaller the line width.

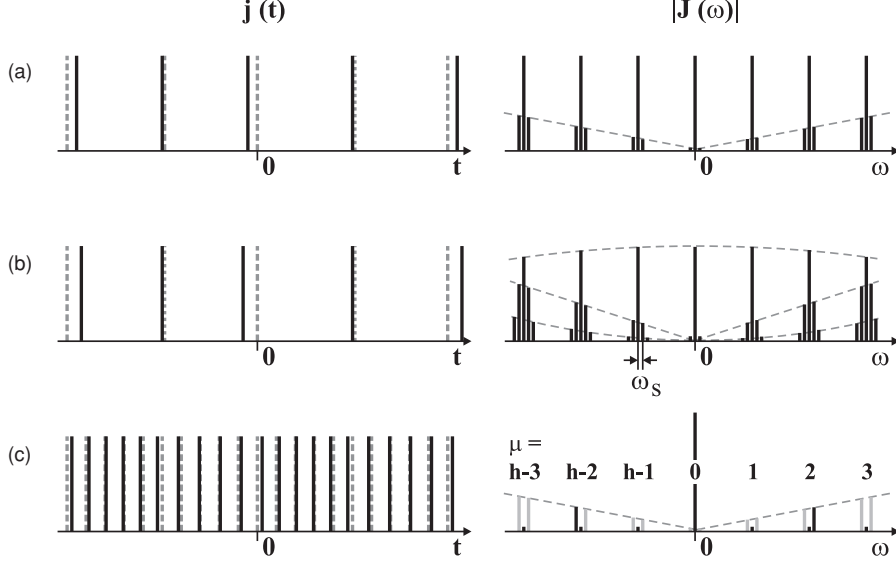


Fig. 2.3. Detected current signal as function of time (*left*) and frequency (*right*) caused by pointlike bunches that oscillate longitudinally with a synchrotron frequency ω_s . (a) Single bunch with small oscillation amplitude and (b) with larger oscillation amplitude, (c) $h = T_o/T_{rf}$ equidistant bunches oscillating with small amplitude. The symbol μ labels a mode with an upper sideband at $\mu\omega_o + \omega_s$

Case 2c. Filling the storage ring with h Gaussian bunches in analogy to case 1c creates a line spectrum consisting of rf harmonics with an envelope given by the Fourier transform of the charge density distribution of the individual bunches. Again, slight variations of the bunch charge cause spurious revolution harmonics, as shown in Fig. 2.2.

2.2.3 Longitudinal Bunch Oscillations

So far, the spacing between electron bunch signals was considered to be equal and time independent. Longitudinal oscillations (“synchrotron oscillations”) modulate the arrival time of the bunches at the detector (see Fig. 2.3).

Case 3a. Consider a pointlike electron bunch circulating in a storage ring with mean revolution frequency ω_o . In the case of a longitudinal motion with frequency ω_s and amplitude $\hat{\tau}$, the current signal is (in arbitrary units)

$$j(t) = \sum_{n=-\infty}^{\infty} \delta(t - nT_o - \hat{\tau} \cos[\omega_s nT_o]) , \quad (2.16)$$

where an arbitrary initial phase of the oscillation was suppressed. For small amplitudes, the spectrum can be expanded:

$$\begin{aligned}
J(\omega) &= \sum_{p=-\infty}^{\infty} \exp(-i\omega\{pT_o + \hat{\tau} \cos[\omega_s pT_o]\}) \\
&\approx \sum_{p=-\infty}^{\infty} (1 - i\omega\hat{\tau} \cos[\omega_s pT_o]) \exp(-i\omega pT_o) \\
&= \sum_{p=-\infty}^{\infty} \exp(-i\omega pT_o) - \frac{i\omega\hat{\tau}}{2} \left[e^{-ipT_o(\omega+\omega_s)} + e^{-ipT_o(\omega-\omega_s)} \right] \\
&= \omega_o \sum_{p=-\infty}^{\infty} \left\{ \delta(\omega - p\omega_o) - \frac{i\hat{\tau}}{2} (p\omega_o - \omega_s) \delta(\omega - p\omega_o + \omega_s) \right. \\
&\quad \left. - \frac{i\hat{\tau}}{2} (p\omega_o + \omega_s) \delta(\omega - p\omega_o - \omega_s) \right\}. \quad (2.17)
\end{aligned}$$

In this approximation, each line at integer multiples of the revolution frequency has a lower and an upper sideband at $p\omega_o \pm \omega_s$. Including one more term into the expansion creates additional small sidebands at $p\omega_o \pm 2\omega_s$.

Case 3b. Without restriction to small oscillation amplitudes, the spectrum is given by

$$J(\omega) = \omega_o \sum_{p=-\infty}^{\infty} \sum_{l=-\infty}^{\infty} i^{-l} \mathcal{J}_l(\hat{\tau}\{p\omega_o + l\omega_s\}) \delta(\omega - p\omega_o - l\omega_s), \quad (2.18)$$

where \mathcal{J}_l are Bessel functions of order l . This result can be obtained from (2.16) using (2.9) and the relation (e.g. [5])

$$\exp(ix \cos \alpha) = \sum_{l=-\infty}^{\infty} i^l \mathcal{J}_l(x) \exp(il\alpha). \quad (2.19)$$

Each line at $p\omega_o$ is now accompanied by a series of sidebands at distance $l\omega_s$ with $l = \pm 1, \pm 2$, and so on. The Bessel function of zeroth order constitutes a finite envelope of the revolution harmonics even if the bunches are assumed to be pointlike. The Bessel functions of order l act as envelopes for the respective sidebands. For small oscillation amplitudes $\hat{\tau}$, expression (2.17) can be recovered from (2.18).

Case 3c. A system of $h = T_o/T_{rf}$ equidistant electron bunches has h eigenmodes $\mu = 0 \dots h-1$ characterized by a phase difference $\Delta\varphi$ between the oscillation of successive bunches³. With just two oscillators, the eigenmodes with $\Delta\varphi = 0$ and π are well known from many examples in physics, e.g. two coupled pendula. For the general case of h oscillators, the phase difference for eigenmode μ is

³ As an intuitive definition, an eigenmode of a system of coupled oscillators is a mode of oscillation that, once excited, continues without beating, i.e. without energy exchange between the oscillators [6].

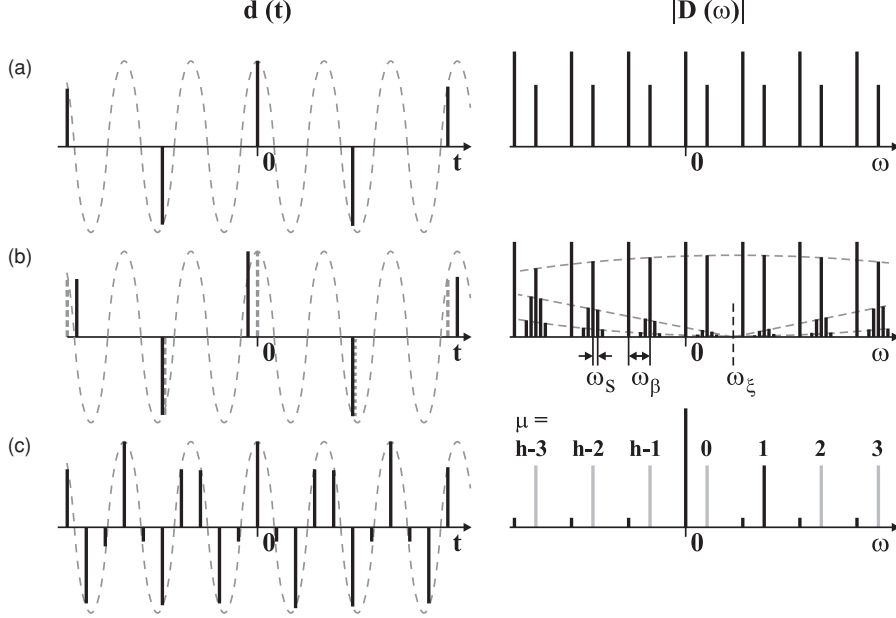


Fig. 2.4. Detected dipole moment as function of time (*left*) and frequency (*right*) for pointlike electron bunches. (a) Single bunch performing transverse oscillations with a betatron frequency ω_β , (b) with additional longitudinal oscillations, (c) $h = T_o/T_{rf}$ equidistant bunches performing transverse oscillations

$$\Delta\varphi = \frac{2\pi\mu}{h} . \quad (2.20)$$

Thus, the revolution harmonic at which the sidebands occur is shifted by the frequency

$$\frac{\Delta\varphi}{\Delta t} = \frac{2\pi\mu}{h} \frac{h}{T_o} = \mu\omega_o , \quad (2.21)$$

since the time difference from bunch to bunch is $\Delta t = T_o/h$. The sideband frequencies are $p\omega_{rf} \pm (\mu\omega_o + \omega_s)$. All h modes are found within a frequency range of $\omega_{rf}/2$, provided the frequency interval starts or ends at an integer multiple of ω_{rf} .

2.2.4 Transverse Bunch Oscillations

In the following discussion of transverse oscillations, $u(t)$ is either the horizontal or the vertical deviation of a bunch from its equilibrium orbit, and quantities like tune, dispersion or chromaticity are understood to carry a subscript x or y .

A detector, which is sensitive to transverse beam motion (see Fig. 2.4), senses a dipole moment given by

$$m(t) = j(t) u(t) , \quad (2.22)$$

where $j(t)$ is the bunch current. Such a detector would also sense the longitudinal motion of bunches due to the variation of their arrival times, whereas a longitudinal detector is not necessarily sensitive to transverse motion.

Case 4a. Let a pointlike bunch in a storage ring perform transverse oscillations (“betatron oscillations”) with amplitude u_β and frequency

$$\omega_\beta = \nu_\beta \omega_\circ = (n_\beta + q_\beta) \omega_\circ, \quad (2.23)$$

where ν_β is the betatron tune, i.e. the number of oscillation periods during one revolution. The integer part of the tune is n_β , the fractional part is q_β . Adding a time-independent deviation u_c by which the beam deviates from the nominal orbit due to small errors of the guiding magnetic fields, the dipole moment (in arbitrary units) as function of time is

$$m(t) = \{u_c + u_\beta \exp(i\omega_\beta t)\} \sum_{n=-\infty}^{\infty} \delta(t - nT_\circ). \quad (2.24)$$

In analogy to the previous examples, the Fourier spectrum is

$$M(\omega) = u_c \omega_\circ \sum_{p=-\infty}^{\infty} \delta(\omega - p\omega_\circ) + u_\beta \omega_\circ \sum_{p=-\infty}^{\infty} \delta(\omega - p\omega_\circ - \omega_\beta). \quad (2.25)$$

The time-independent deviation results in a spectrum of revolution harmonics $p\omega_\circ$, whereas the betatron motion creates new lines displaced by $+\omega_\beta$ with respect to the revolution harmonics. In the measurable spectrum, i.e. the combination of positive and negative frequencies, there are two betatron lines between each pair of adjacent revolution harmonics. Their distance to the closest revolution harmonic is $\pm q'_\beta \omega_\circ$ with $q'_\beta < 0.5$. This observation is ambiguous in two ways:

- The integer part of the tune cannot be deduced since the detector installed at one position of the storage ring is insensitive to the integer number of cycles between two observations (alias effect).
- The fractional part of the tune could be $q_\beta = q'_\beta$ or $q_\beta = 1 - q'_\beta$. This ambiguity can be experimentally removed by increasing the field of a focussing quadrupole magnet, which causes the tune to rise. If the distance q'_β increases, then $q_\beta = q'_\beta$.

Case 4b. Let a pointlike, transversely oscillating bunch perform additional longitudinal oscillations with synchrotron frequency ω_s . This modifies the spectrum in several ways:

1. The arrival time of the bunch at the detector is modulated.
2. A longitudinal oscillation is also an oscillation in energy. If $\delta_E(t)$ denotes the relative deviation from the nominal beam energy, then
 - the transverse bunch position changes according to $D \delta_E(t)$ in a region with dispersion $D \neq 0$.

- the betatron tune is modulated by the energy oscillation if the chromaticity $\xi = d\nu_\beta/d\delta_E$ is non-zero.

Quantitatively, (A.32) and (A.33) show that an oscillation of the bunch arrival time $\tau = \hat{\tau} \cos(\omega_s t)$ corresponds to an energy oscillation $\delta_E(t) = \dot{\tau}/\eta = -(\omega_s \hat{\tau}/\eta) \sin(\omega_s t)$ with η being the momentum compaction factor. The dipole moment is then

$$m(t) = \left\{ u_c - D \frac{\omega_s \hat{\tau}}{\eta} \sin(\omega_s t) + u_\beta \exp(i\phi_\beta(t)) \right\} \times \sum_{n=-\infty}^{\infty} \delta(t - nT_o - \hat{\tau} \cos[\omega_s nT_o]) . \quad (2.26)$$

Here, the betatron motion is expressed by its phase advance $\phi_\beta(t)$ with

$$\dot{\phi}_\beta(t) = \omega_\beta + \Delta\omega_\beta(t) = \omega_\beta + \omega_o \xi \delta_E(t) = \omega_\beta + \frac{\omega_o \xi \dot{\tau}(t)}{\eta} . \quad (2.27)$$

Integration yields

$$\phi_\beta(t) = \phi_\beta(0) + \omega_\beta t + \frac{\omega_o \xi \tau(t)}{\eta} = \phi_\beta(0) + \omega_\beta t + \omega_\xi \hat{\tau} \cos(\omega_s t) , \quad (2.28)$$

where the so-called chromatic frequency $\omega_\xi = \omega_o \xi/\eta$ is introduced. The first term of (2.26) leads to synchrotron sidebands as in (2.18). The second term, which vanishes in dispersion-free regions, also creates sidebands at a distance $\pm l\omega_s$ from the revolution harmonics, but their envelopes differ from those of the first term. The third term gives rise to new lines in the spectrum. Its Fourier transform is given by [2]

$$M(\omega) = \omega_o u_\beta \sum_{p=-\infty}^{\infty} \sum_{l=-\infty}^{\infty} i^{-l} \mathcal{J}_l(\hat{\tau}\{p\omega_o + \omega_\beta + l\omega_s - \omega_\xi\}) \times \delta(\omega - p\omega_o - \omega_\beta - l\omega_s) . \quad (2.29)$$

Thus, the energy dependence of the betatron frequency due to chromaticity creates two new phenomena:

- Not only the revolution harmonics but also the betatron lines are accompanied by synchrotron sidebands.
- The envelope of these sidebands is shifted by the chromatic frequency $\omega_\xi = \omega_o \xi/\eta$.

Case 4c. For $h = T_o/T_{rf}$ equidistant electron bunches executing transverse oscillations, there are h eigenmodes labeled $\mu = 0 \dots h-1$. As in the longitudinal case, they are characterized by a phase difference

$$\Delta\varphi = \frac{2\pi\mu}{h} , \quad (2.30)$$

between successive bunches and the frequencies of the betatron sidebands are $\omega = p\omega_{\text{rf}} + \mu\omega_o + \omega_\beta$. As in the longitudinal case, a measuring apparatus that does not distinguish between positive and negative frequencies, and all h transverse modes are found within a frequency interval of $\omega_{\text{rf}}/2$, provided it starts or ends at an integer multiple of ω_{rf} .

Since bunches were treated as pointlike or at least rigid objects without inner degrees of freedom, the results obtained here reappear in the context of one-particle models for multi-bunch instabilities.

Figure 2.5 shows examples of beam spectra recorded at the storage ring BESSY II using a spectrum analyzer. The central frequency was kept fixed at twice the rf frequency while the frequency span was reduced by a zoom factor of 250 from one spectrum to the next.

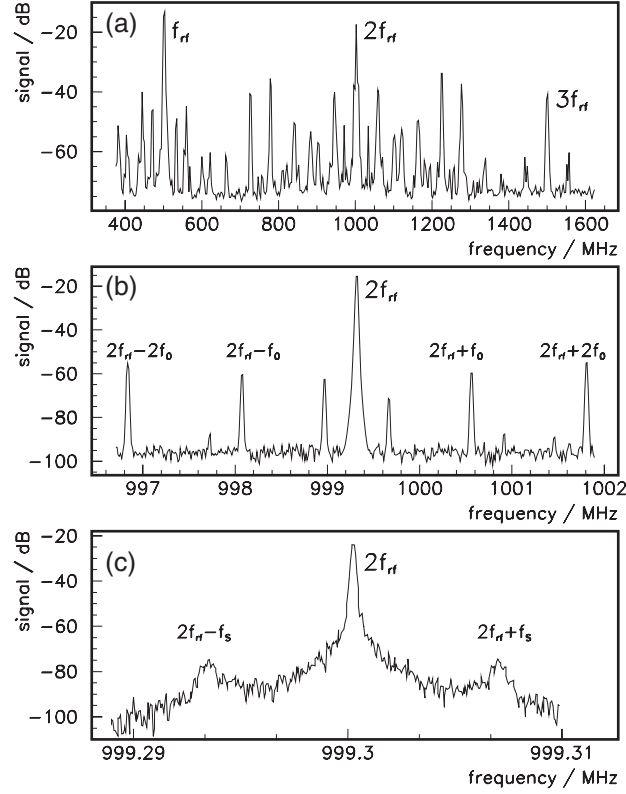


Fig. 2.5. Spectra of an unstable electron beam in BESSY II. In each case, the central frequency coincides with 999.3 MHz, which is twice the rf frequency f_{rf} . At a GHz span (a) groups of lines between the integer multiples of f_{rf} indicate the presence of instabilities; on a MHz scale (b) betatron sidebands between integer multiples of the revolution frequency f_o are visible, on the kHz scale (c) synchrotron sidebands are resolved

In order to decide whether the beam is stable or not, the span of the spectrum analyzer must cover all possible mode frequencies, i.e. at least half the rf frequency. Whether a line in the spectrum corresponds to a longitudinal or transverse oscillation is determined by measuring its frequency difference to an adjacent revolution harmonic, which either matches the synchrotron frequency or the product of fractional betatron tune and revolution frequency. For a storage ring filled with many bunches, the revolution harmonics may not even be visible (spurious revolution harmonics are more pronounced in the vicinity of rf harmonics) and its frequency must be carefully calculated from the known rf frequency – for kHz accuracy of the result, even the 1-Hz digit of the rf frequency should be included.

2.3 Wake Field and Impedance

In agreement with the majority of the literature (e.g. [7–11]), the following terms are introduced:

- *Wake field* is the electromagnetic field caused by an arbitrary charge distribution interacting with its surroundings.
- *Wake function* is the integral over time of the force caused by a pointlike unit charge and acting via wake fields on a pointlike trailing unit charge.
- *Wake potential* is the integral over time of the force caused by an extended unit charge and acting via wake fields on a pointlike trailing unit charge.
- *Impedance* is the Fourier transform of the wake function.

2.3.1 Longitudinal and Transverse Wake Function

Consider the situation displayed in Fig. 2.6: Two charges travel at almost the speed of light $\mathbf{v} \approx (0, 0, c)$ in the vacuum chamber of a storage ring. Let the coordinates of the leading charge q_1 and the trailing charge q_2 at a given time t be (\mathbf{r}_1, s_1) and (\mathbf{r}_2, s_2) , respectively. The interaction of the leading charge

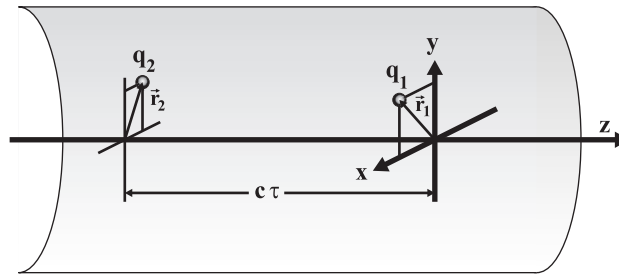


Fig. 2.6. Two charges q_1 and q_2 with transverse position vectors \mathbf{r}_1 and \mathbf{r}_2 , respectively, travelling in a vacuum chamber. The distance between leading and trailing charge, measured along the z -axis, is $c\tau$

with the vacuum chamber causes an electromagnetic wake field that results in a force

$$\mathbf{F}(\mathbf{r}_1, s_1, \mathbf{r}_2, s_2, t) = q_2 \{ \mathbf{E}(\mathbf{r}_1, s_1, \mathbf{r}_2, s_2, t) + \mathbf{v} \times \mathbf{B}(\mathbf{r}_1, s_1, \mathbf{r}_2, s_2, t) \} \quad (2.31)$$

on the trailing charge. Assuming the force to be sufficiently weak, both charges maintain a nearly uniform motion characterized by a constant distance $c\tau = s_1(t) - s_2(t)$. In order to study the effect of a given structure (an rf cavity, for example) on a particle beam, it is sufficient to specify the time integral of the force, normalized to the values of both charges, as a function of the distance between them:

$$\mathbf{W}(\mathbf{r}_1, \mathbf{r}_2, \tau) = -\frac{c}{q_1} \int dt \{ \mathbf{E}(\mathbf{r}_1, \mathbf{r}_2, \tau, t) + \mathbf{v} \times \mathbf{B}(\mathbf{r}_1, \mathbf{r}_2, \tau, t) \} . \quad (2.32)$$

This is the wake function, the longitudinal part of which corresponds to the energy change ΔU experienced by the trailing charge under the influence of the wake field, normalized to the charges:

$$W_{\parallel}(\mathbf{r}_1, \mathbf{r}_2, \tau) = -\frac{\Delta U}{q_1 q_2} = -\frac{c}{q_1} \int dt E_z(\mathbf{r}_1, \mathbf{r}_2, \tau, t). \quad (2.33)$$

The unit of W_{\parallel} is V/C. By convention, the minus sign makes the wake function positive for negative energy changes, i.e. energy loss. In the longitudinal case, there is no magnetic term, because $\mathbf{v} \times \mathbf{B}$ has no longitudinal component. The transverse wake function is

$$\mathbf{W}_{\perp}(\mathbf{r}_1, \mathbf{r}_2, \tau) = -\frac{c}{q_1} \int dt \{ \mathbf{E}_{\perp}(\mathbf{r}_1, \mathbf{r}_2, \tau, t) + [\mathbf{v} \times \mathbf{B}(\mathbf{r}_1, \mathbf{r}_2, \tau, t)]_{\perp} \} \quad (2.34)$$

and with this particular definition, the unit of \mathbf{W}_{\perp} is J C⁻² or V C⁻¹. In the ultrarelativistic case considered here, the wake function is zero for negative values of τ due to causality. In the literature, \mathbf{W} may also be defined as function of the distance d with $\mathbf{W}(d < 0) = 0$ or as function of the coordinate z in flight direction with the leading charge at $z = 0$, which implies $\mathbf{W}(z > 0) = 0$.

Sometimes, the transverse wake function is not normalized to the charge q_1 but to the dipole moment for a given horizontal or vertical offset of the leading charge, while $\mathbf{r}_2 = 0$. In this case, its unit is V C⁻¹ m⁻¹:

$$W_{uv}(\tau) = -\frac{c}{q_1 u} \int \{ \mathbf{E}_v(u, 0, \tau, t) + [\mathbf{v} \times \mathbf{B}(u, 0, \tau, t)]_v \} , \quad (2.35)$$

where $u = x$ or $u = y$ is the offset of q_1 and the subscript $v = x$ or $v = y$ indicates the field component under consideration. Mixed terms with $u = x$ and $v = y$ or $u = y$ and $v = x$ vanish if the vacuum chamber has rotational symmetry about the beam axis. If the vacuum chamber has no obvious symmetry, the dipole moments are not meaningful and (2.34) should be used.

In the case of rotational symmetry, a multipole expansion in cylindrical coordinates with unit vectors $\hat{r}, \hat{\theta}$ is advantageous. Defining $\theta \equiv \theta_2 - \theta_1$, the longitudinal and transverse wake functions are

$$\begin{aligned} W_{\parallel}(r_1, r_2, \theta, \tau) &= \sum_{m=0}^{\infty} \frac{2}{1 + \delta_{m0}} r_1^m r_2^m \cos m\theta W_{\parallel}^{(m)}(\tau) \\ W_{\perp}(r_1, r_2, \theta, \tau) &= \sum_{m=1}^{\infty} r_1^{m-1} r_2^m \left[\hat{r} \cos m\theta - \hat{\theta} \sin m\theta \right] W_{\perp}^{(m)}(\tau) . \end{aligned} \quad (2.36)$$

In this definition, the units of the longitudinal multipole components are $\text{V C}^{-1} \text{m}^{-2m}$ and the units of the transverse multipole components are $\text{V C}^{-1} \text{m}^{-2m+1}$. The transverse displacement r of a particle is often assumed to be small compared to the chamber radius R , and, according to dimensionality arguments, the higher orders decrease roughly like $(r/R)^{2m}$. Thus, for practical purposes, only the lowest-order terms are of interest:

- Longitudinal wake function $W_{\parallel} \approx W_{\parallel}^{(0)} (\text{V C}^{-1})$
- Transverse wake function $W_{\perp} \approx W_{\perp}^{(1)} (\text{V C}^{-1} \text{m}^{-1})$

In the ultrarelativistic case, the longitudinal wake function is independent of the transverse position r_2 of a hypothetical test charge. This fact is used to simplify the numerical determination of the wake potential (see Sect. 2.3.5).

2.3.2 Extended Charge Distribution: Wake Potential

The consideration of extended charge distributions is motivated by the fact that the size of real particle bunches usually cannot be neglected. Furthermore, the time-domain simulation of wake fields on a spatial and temporal grid requires the bunch charge to be distributed over several grid points. Such a simulation cannot directly determine the wake function, which is defined for point charges.

Starting from the longitudinal wake function $W_{\parallel}(t)$, the superposition principle yields the wake potential for a longitudinally extended charge distribution $j(\tau)$:

$$V_{\parallel}(\tau) = \int_{-\infty}^{\infty} dt W_{\parallel}(t) j(\tau - t) . \quad (2.37)$$

Assuming a transverse displacement $u(\tau)$ with mean value $\langle u \rangle$, the transverse wake potential is defined as

$$V_{\perp}(\tau) = \frac{1}{\langle u \rangle} \int_{-\infty}^{\infty} dt W_{\perp}(t) u(\tau - t) j(\tau - t) . \quad (2.38)$$

If the transverse displacement is constant along the bunch, the previous expression reduces to

$$V_{\perp}(\tau) = \int_{-\infty}^{\infty} dt W_{\perp}(t) j(\tau - t) . \quad (2.39)$$

Generally, a wake potential is obtained by a convolution of wake function and charge distribution. Its Fourier transform is just the product of the Fourier transforms of the convoluted functions. This can be used to recover the wake function from the wake potential obtained by numerical simulations (see Sect. 2.3.5).

2.3.3 Longitudinal and Transverse Impedance

The Fourier transform of the respective wake function

$$Z_{\parallel}(\omega) = \int_{-\infty}^{\infty} d\tau W_{\parallel}(\tau) \exp(-i\omega\tau), \quad (2.40)$$

$$Z_{\perp}(\omega) = i \int_{-\infty}^{\infty} d\tau W_{\perp}(\tau) \exp(-i\omega\tau) \quad (2.41)$$

is the longitudinal or transverse impedance (or “coupling impedance”). Following the usual convention, the definition of the transverse impedance includes a phase factor $i = \exp(i\pi/2)$, because the betatron oscillation transforms the kick from a transverse force into a transverse displacement after a phase advance of $\pi/2$. The notion of impedance was introduced to accelerator physics in the 1960s [12, 13]. To illustrate the analogy to the impedance used in electrical engineering, one may insert

$$j(\tau) = \frac{1}{2\pi} \int_{-\infty}^{\infty} d\omega J(\omega) \exp(i\omega\tau) \quad (2.42)$$

into (2.37) expressing the longitudinal wake potential as

$$\begin{aligned} V_{\parallel}(\tau) &= \int_{-\infty}^{\infty} dt W_{\parallel}(t) \frac{1}{2\pi} \int_{-\infty}^{\infty} d\omega J(\omega) \exp(i\omega\tau - i\omega t) \\ &= \frac{1}{2\pi} \int_{-\infty}^{\infty} d\omega Z_{\parallel}(\omega) J(\omega) \exp(i\omega\tau) . \end{aligned} \quad (2.43)$$

On the other hand, the wake potential is the Fourier transform of $\tilde{V}_{\parallel}(\omega)$

$$V_{\parallel}(\tau) = \frac{1}{2\pi} \int_{-\infty}^{\infty} d\omega \tilde{V}_{\parallel}(\omega) \exp(i\omega\tau) . \quad (2.44)$$

Comparison with (2.43) yields an expression that is analogous to Ohm’s law:

$$\tilde{V}_{\parallel}(\omega) = Z_{\parallel}(\omega) J(\omega) . \quad (2.45)$$

Thus, in the frequency domain the impedance connects a current distribution $J(\omega)$ to the voltage $\tilde{V}(\omega)$ induced by its wake field. On the other hand,

one may use this as a definition of the impedance and show that it is the Fourier transform of the wake function. Analogous impedance concepts exist for the description of mechanical and acoustic waves [4]. In either case, the impedance is a complex function of frequency and its real part describes dissipative effects:

- electrically through resistance according to Ohm’s law
- for mechanical systems through friction.

Its imaginary part is responsible for retarding effects or phase shifts:

- between an electric current and voltage via inductance and capacitance
- between a mechanical generator and an oscillator due to inertia.

2.3.4 Properties of Wake Function and Impedance

The Panofsky–Wenzel Theorem

There is a simple relationship between longitudinal and transverse wake function, known as the Panofsky–Wenzel theorem [14]:

$$\frac{1}{c} \frac{\partial}{\partial \tau} \mathbf{W}_\perp(\mathbf{r}_1, \tau) = -\nabla_\perp W_\parallel(\mathbf{r}_1, \tau) . \quad (2.46)$$

The time-derivative of the transverse wake function can be calculated from the transverse variation of the longitudinal wake function. In the frequency domain, the theorem also states that the transverse impedance can be calculated from the longitudinal impedance:

$$\mathbf{Z}_\perp(\mathbf{r}_1, \omega) = \frac{c}{\omega} \nabla_\perp Z_\parallel(\mathbf{r}_1, \omega) . \quad (2.47)$$

Originally formulated for geometrical structures with rotational symmetry, the Panofsky–Wenzel theorem is also valid for other geometries [15]. While the Panofsky–Wenzel theorem applies to each multipole order m separately, there is no simple connection between different multipole components. However, the multipole orders of the impedance for a vacuum chamber of radius R can be assumed to decrease roughly like

$$Z_\parallel^{(m)} \approx \frac{2}{R^{2m}} Z_\parallel^0 \quad (2.48)$$

and applying the Panofsky–Wenzel theorem

$$Z_\perp^{(m)} \approx \frac{2c}{\omega R^{2m}} Z_\parallel^0 . \quad (2.49)$$

Here, a factor of two was inserted arbitrarily to be consistent with (2.57) and (2.58) that hold for the resistive-wall impedance (see Sect. 2.3.5).

Narrow-Band Resonators

In analogy to an LRC resonator circuit, the impedance of cavity-like structures is often assumed to be of the form

$$Z_{\parallel}(\omega) = \frac{R_s}{1 + iQ(\omega_r/\omega - \omega/\omega_r)}, \quad (2.50)$$

$$Z_{\perp}(\omega) = \frac{c}{\omega} \frac{R_s}{1 + iQ(\omega_r/\omega - \omega/\omega_r)}. \quad (2.51)$$

In this case, the impedance is determined by the resonant frequency ω_r , the shunt impedance R_s and the quality factor Q . Fourier transform yields the wake functions, given here in the approximation of a weakly damped resonator ($Q \gg 1$):

$$W_{\parallel}(\tau) \approx \frac{\omega_r R_s}{Q} e^{-\omega_r \tau / 2Q} \cos(\omega_r \tau) \quad (\tau > 0), \quad (2.52)$$

$$W_{\perp}(\tau) \approx -\frac{c R_s}{Q} e^{-\omega_r \tau / 2Q} \sin(\omega_r \tau) \quad (\tau \geq 0). \quad (2.53)$$

Apparently, the derivative of the transverse wake function is proportional to the longitudinal wake function. This can be shown to be generally true by analyzing Maxwell's equations for rotationally symmetric boundary conditions [7].

Properties of the Wake Function

Some general properties of longitudinal wake functions $W_{\parallel}(\tau)$ and transverse wake functions $W_{\perp}(\tau)$ are summarized in the following and illustrated by Fig. 2.7. See e.g. [7,8] for detailed derivations. The symbols $\tau = 0^+$ and $\tau = 0^-$ represent infinitesimally small positive and negative time values.

- (a) $W_{\parallel}(0^-) = 0$ and $W_{\perp}(0^-) = 0$ for ultrarelativistic particles. This property, also referred to as “causality”, is due to the fact that electromagnetic fields cannot propagate faster than a charge travelling approximately at the speed of light.

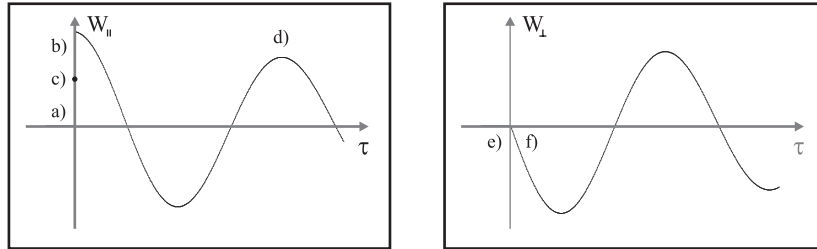


Fig. 2.7. Schematic illustration of longitudinal (*left*) and transverse (*right*) wake function versus time τ indicating the properties (a)–(f) as discussed in the text

- (b) $W_{\parallel}(0^+) \geq 0$. According to the definition (2.33), a positive value corresponds to energy loss. A charged particle cannot gain energy from its own field by traversing a passive structure.
- (c) $W_{\parallel}(0) = \frac{1}{2}W_{\parallel}(0^+)$, often called the “fundamental theorem of beam loading”, implies that a charge is retarded by its own wake field, but sees only half of it (see also Appendix D).
- (d) $W_{\parallel}(0^+) \geq |W_{\parallel}(\tau)|$. In the limit $W_{\parallel}(0^+) = |W_{\parallel}(\tau)|$, the maximum repeats itself with a period τ , corresponding to the wake caused by a resonator with infinitely large quality factor.
- (e) $W_{\perp}(0) = 0$, a charge is not transversely displaced by its own wake field. This and the following property can be shown from the longitudinal wake function being proportional to the derivative of the transverse wake function.
- (f) $W_{\perp}(0^+) < 0$. Furthermore, maxima of W_{\perp} coincide with zero crossings of W_{\parallel} . In summary, one may say that the transverse wake function is sine-like and the longitudinal wake function is cosine-like.

Properties of the Impedance

The fact that a wake function is real and vanishes for $\tau < 0$ imposes some restrictions on its Fourier transform, the impedance (see Fig. 2.8).

- (a) $Z_{\parallel}^*(\omega) = Z_{\parallel}(-\omega)$ and $Z_{\perp}^*(\omega) = -Z_{\perp}(-\omega)$, where the asterisk indicates the complex conjugate value. Furthermore, $Z_{\parallel}(0) = 0$ and $\text{Re}Z_{\perp}(0) = 0$.
- (b) $\text{Re}Z_{\parallel}(\omega) \geq 0$ for all ω , whereas $\text{Re}Z_{\perp}(\omega) \geq 0$ for $\omega > 0$ and $\text{Re}Z_{\perp}(\omega) \leq 0$ for $\omega < 0$.
- (c) The real and imaginary parts of the impedance are not independent from each other, but are connected by a Hilbert transform [4]. For the resonator impedance at $\omega \neq 0$, the peaks of the real part coincide with zero crossings of the imaginary part.
- (d) To calculate the wake function from the impedance, it is sufficient to know its real or imaginary part, e.g.:

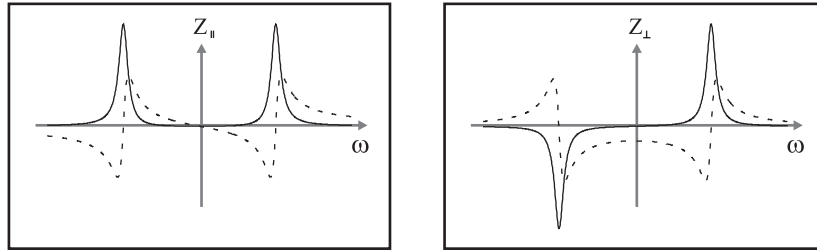


Fig. 2.8. Schematic illustration of longitudinal (*left*) and transverse (*right*) impedance versus frequency ω , where the *solid line* represents the real part and the *dashed line* is the imaginary part of the complex impedance

<http://www.springer.com/978-3-540-34312-7>

Collective Phenomena in Synchrotron Radiation
Sources

Prediction, Diagnostics, Countermeasures

Khan, S.

2006, X, 203 p., Hardcover

ISBN: 978-3-540-34312-7